Earth and Planetary Science Letters 395 (2014) 13–23

Contents lists available at ScienceDirect

Earth and Planetary Science Letters

www.elsevier.com/locate/epsl

The preservation of $\delta^{34}S_{SO_4}$ and $\delta^{18}O_{SO_4}$ in carbonate-associated sulfate during marine diagenesis: A 25 Myr test case using marine sediments

Victoria C.F. Rennie *, Alexandra V. Turchyn

University of Cambridge, Department of Earth Sciences, Cambridge, United Kingdom

ARTICLE INFO

Article history:
Received 20 June 2013
Received in revised form 12 March 2014
Accepted 13 March 2014
Available online 3 April 2014
Editor: G.M. Henderson

Keywords:
carbonate-associated sulfate
carbonate recrystallization
sulfur isotopes
oxygen isotopes
diagenesis
Ocean Drilling Program

ABSTRACT

A 25 million year record of the sulfur and oxygen isotope composition of marine carbonate-associated sulfate (CAS) was constructed from 55 nannofossil ooze samples at three different locations. We tested the impact of early marine diagenesis on CAS by comparing the CAS extractions to the sulfur and oxygen isotope composition of the associated pore fluid sulfate, to determine the degree of pore fluid incorporation during carbonate recrystallization. Neither the sulfur nor the oxygen isotope composition of CAS are completely overprinted by incorporation of pore fluid sulfate. We compare our record to the sulfur and oxygen isotope records of coeval barite. The sulfur isotope record is in agreement with the barite record within ±2‰, except where very young (<2 Ma) sediments are in the presence of highly evolved pore fluid sulfate ($\delta^{34}S = 70‰$). A simple recrystallization model is used to illustrate the sensitivity of CAS $\delta^{34}S_{SO_4}$ to sedimentation rate, and to emphasize that careful sample selection, along with an analysis of early diagenetic environmental conditions is crucial when interpreting CAS sulfur isotopes. Oxygen isotopes in CAS are more complex and do not reproduce similar values to those of coeval barite. We conclude that oxygen isotopes in sulfate may remain a useful proxy but merit closer attention in the future.

1. Introduction

The marine biogeochemical sulfur cycle has played a critical role in the evolution of Earth's surface environment (Holland, 1984). The concentration of sulfate in the ocean reflects the balance between the terrestrial weathering of sulfur-bearing minerals and the burial of sulfur as evaporites and sedimentary sulfides in the oceans (Holser et al., 1988; Berner and Canfield, 1989). Sulfate reduction to sulfide occurs principally through bacterial sulfate reduction, which comprises a significant portion of anaerobic carbon oxidation in marine sediments (Kasten and Jørgensen, 2000). The subsequent burial of sulfide as pyrite is further understood to be an indirect source of oxygen to the atmosphere (Berner, 1987). Thus, reconstructing the relative fluxes of weathering versus burial within the marine sulfur cycle may yield critical insight into the evolution of both the carbon cycle and the oxidation state of Earth's surface (Berner, 1987; Canfield, 2005).

The sulfur and, more recently, oxygen isotope composition of sulfur-bearing minerals precipitated in the ocean ($\delta^{34}S_{SO_4}$ and $\delta^{18}O_{SO_4}$ respectively) are the primary tools used for reconstructing the various fluxes within the marine sulfur cycle over geological time (Claypool et al., 1980; Canfield, 1998; Paytan et al., 1998, 2004; Newton et al., 2004). While traditionally the $\delta^{34}S_{SO_4}$ and $\delta^{18}O_{SO_4}$ have been measured in evaporite minerals and barium sulfate (barite), over the last 20 years a new mineral proxy for the sulfur cycle has been increasingly used: carbonate-associated sulfate (CAS) (e.g. Burdett et al., 1989; Kampschulte et al., 2001; Hurtgen et al., 2002; Kah et al., 2004; Kampschulte and Strauss, 2004; Newton et al., 2004; Gellatly and Lyons, 2005; Gill et al., 2005, 2007; Fike and Grotzinger, 2008). CAS is sulfate that has been incorporated into carbonate minerals upon precipitation, substituting for a carbonate ion in the mineral lattice (Takano, 1985; Pingitore et al., 1995). Whilst questions remain as to the mechanism of sulfate incorporation into carbonate minerals, CAS has been shown to record the isotopic composition of sulfate of the coeval seawater with no apparent fractionation for either $\delta^{18}O_{SO_4}$ (Cortecci and Longinelli, 1971; Newton et al., 2004) or $\delta^{34}S_{SO_4}$ (Burdett et al., 1989; Kampschulte et al., 2001; Kampschulte and Strauss, 2004).

Palaeoproxies extracted from carbonate minerals and rocks have significant advantages over other mineral proxies, namely the almost ubiquitous presence of carbonate rocks over geological time, and with it the potential for high temporal resolution. This continuity of the carbonate rock record is in contrast to

* Corresponding author.
E-mail address: vcr22@cam.ac.uk (V.C.F. Rennie).

http://dx.doi.org/10.1016/j.epsl.2014.03.025

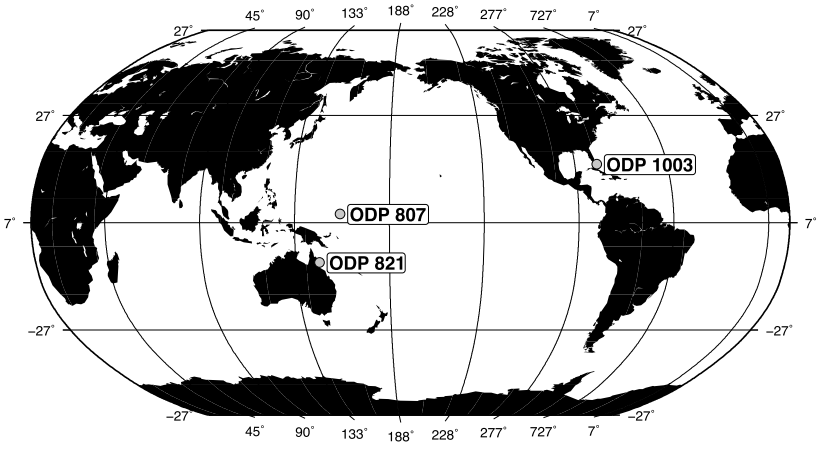

Fig. 1. Map of the three study sites.

the discontinuous evaporite record, and the marine barite record, which is limited to the last ~130 Ma. However, the use of carbonate minerals as paleoproxies for seawater chemistry is limited by their susceptibility to recrystallization during marine diagenesis, broadly termed 'diagenetic overprinting' (e.g. Fantle et al., 2010). This diagenetic overprinting refers to the rapid dissolution and reprecipitation of carbonate minerals in the youngest, uppermost sediments, and the possibility that during this recrystallization, the primary geochemical signatures of the carbonates are either modified or lost.

Early diagenetic overprinting in marine sediments may be a significant obstacle for CAS as a proxy for the marine sulfur cycle. When carbonate minerals recrystallize within marine sediments, they do so in contact with pore fluids that may have a significantly different sulfur and oxygen isotope composition of sulfate than seawater (e.g. Fritz et al., 1989; Wortmann et al., 2007). Bacterial sulfate reduction in sediments results in the pore fluid sulfate becoming enriched in ^{34}S and ^{18}O (e.g. Mizutani and Rafter, 1973; Brunner et al., 2005; Wortmann et al., 2007). The recrystallization of sedimentary carbonate under these conditions could result in the incorporation of isotopically distinct sulfate into the recrystallized carbonate, which would potentially overprint the primary (seawater) $\delta^{18}O_{SO_4}$ and $\delta^{34}S_{SO_4}$.

In carbonates with high original sulfate concentrations, CAS $\delta^{18}O_{SO_4}$ and $\delta^{34}S_{SO_4}$ are likely buffered against significant diagenetic overprinting. This is particularly the case where the diagenetic fluid has very low sulfate concentrations, such as meteoric fluids (Gill et al., 2008), but CAS $\delta^{34}S_{SO_4}$ may also be unaffected by diagenesis in contact with sulfate-rich fluids. For example, Lyons et al. (2004) demonstrated that CAS $\delta^{34}S_{SO_4}$ remained unchanged in carbonate-rich sediments of the Florida Keys, despite extensive authigenic carbonate precipitation in the presence of bacterial sulfate reduction. The high sulfate concentrations in the original carbonate, in this case lime muds (2400–4200 ppm CAS), likely 'buffered' the CAS to any diagenetic overprinting (analogous to strontium isotopes, which are also considered to be buffered during carbonate recrystallization – e.g. Baker et al., 1982; Richter and DePaolo, 1987). The Florida Keys sediments, however, may not be representative of the full suite of carbonates rocks often used for CAS extraction. The range of CAS concentrations in biogenic carbonate can be as high as 20 000 ppm, but in foraminifera and coccoliths CAS concentrations are typically lower than 1000 ppm, and commonly as low as 600 ppm (Staudt and Schoonen, 1995). Furthermore, while the Florida Keys sediments had significant authigenic, or *in situ* carbonate precipitation, it is unknown how they would evolve on timescales of a few million years while undergoing carbonate recrystallization (dissolution and reprecipitation).

In this paper, we investigate the effect of early marine diagenesis on carbonate sediments by comparing isotope data from coexisting pore fluids and minerals for both $\delta^{18}O_{SO_4}$ and $\delta^{34}S_{SO_4}$. We present data from three carbonate-rich sediments collected during the Ocean Drilling Program, chosen for their range of bacterial sulfate reduction and sedimentation rates. The sediment ages span 0–25 Ma, which encompasses the critical timescale over which maximum recrystallization is expected to occur (carbonate recrystallization rates in near surface sediments can be as much as a few percent per million years, and much higher in the very youngest sediment – Maher et al., 2004, 2006; Fantle and DePaolo, 2007). Our results are directly compared with the coeval barite $\delta^{18}O_{SO_4}$ and $\delta^{34}S_{SO_4}$ records, to assess the viability of CAS as a proxy for both $\delta^{18}O_{SO_4}$ and $\delta^{34}S_{SO_4}$. We use a simple model to pinpoint the conditions in which recrystallization may overprint CAS. We then apply the model to two of the sites to obtain rough estimates of recrystallization rates. We discuss the implications of our findings for the use of CAS in the geological record.

2. Sample sites

All three studied sites (Fig. 1) are carbonate rich and show varying degrees of bacterial sulfate reduction. Site 807 (Ontong-Java Plateau) is the deepest site, at a water depth of 2815 m. The sediment is ~90 wt% carbonate, comprising nanofossil and foraminiferal ooze, which overlies nanofossil chalk at 293 m below the sea floor (mbsf). Total organic carbon varies between 0.02 and 0.6%. The sediment pile is estimated to be ~1380 m thick, overlying a 40 km thick ocean crust. Sedimentation rates in the uppermost 600 m are on average 15 m Myr^{-1}, except in the late Miocene (8–5 Ma, ~175 mbsf) where they increase to 40 m Myr^{-1}. Pore fluid sulfate concentrations drop from seawater values (28 mM) to 22 mM in the top 100 m (Shipboard Scientific Party, 1991a). Carbonate recrystallization rates at Site 807 have been extensively studied using strontium, calcium, and magnesium concentrations and isotopes (Fantle and DePaolo, 2006, 2007; Higgins and Schrag, 2012).

Site 1003 is on the Bahama Bank in the Atlantic, with a water depth of 490 m. Coring recovered a full Neogene-Recent sequence, comprising 1300 m of sediment. The uppermost 200 m of sediments recovered at this Site are Pliocene-Recent in age, and are 90 wt% carbonate, from both mixed pelagic and bank-derived carbonates. The sediment is predominantly unlithified packstones, with abundant *Halimeda* debris, intercalated with unlithified and bioturbated mudstones. Sedimentation is thought to be continuous

in this upper 200 m, but rates increase at ~110 mbsf (corresponding with the Plio-Pleistocene transition) from 25 m Myr^{-1} to ~100 m Myr^{-1}. The carbonate mineralogy is dominated by high magnesium calcite and dolomite at 100–200 mbsf, and by aragonite and high magnesium calcite above 100 mbsf. Total organic carbon is <1%, except for one horizon of 2 wt% organic carbon at 100 m depth. Pore fluid sulfate concentrations remain near seawater values for the top 50 m, where they then decrease to 15 M by 100 mbsf (Shipboard Scientific Party, 1997).

Site 821 is the shallowest of the three studied sites. It is situated on the Eastern Australian continental slope with a water depth of 212 m. The sediment at this Site is composed of siliclastic sands and muds, interbedded with calcerous clays (40–70% carbonate), and total organic carbon in the sediment varies between 0.15 and 0.45%. Four hundred metres of sediment were recovered at this site, spanning the last 2 Ma. The sediment column is comprised of three progradational packets, overlain by two aggradational sedimentary sequences, with one hypothesised hiatus between the uppermost two sequences. The base of the sediment column was not reached during coring, but the sediment packet is estimated to be ~1000 m thick in total, from previous seismic surveys (Symonds et al., 1983). Sedimentation rates in the recovered section are high compared to the other sites in this study – varying between 100 m Myr^{-1} (at the very top of the sediment column) to 500 m Myr^{-1} at 80 m depth, with an average sedimentation rate of ~200 m Myr^{-1}. Pore fluid sulfate concentrations at Site 821 drop steadily from seawater values to 1 mM over the top 150 m.

3. Methods

3.1. Pore fluid sulfate extraction

Pore fluid sulfate was precipitated as barite by addition of a saturated $BaCl_2$ solution. The resulting $BaSO_4$ was cleaned of possible $BaCO_3$ contamination by addition of 2 ml 6 M HCl. Samples were agitated and then left in acid for a few hours before removing the supernatant, and rinsing twice in 18.2 MΩ water. Samples were then dried and prepared for analysis of $\delta^{34}S_{SO_4}$ and $\delta^{18}O_{SO_4}$.

3.2. Carbonate-associated sulfate

Ten–twenty grams of sediment were analysed for carbonate-associated sulfate using a method adapted from Burdett et al., 1989. Samples were homogenized and rinsed for 24 hr in 30% NaCl solution to remove any soluble sulfates. This was followed by a further 24 hr in 5% NaOCl in order to oxidise and remove any organic-bound sulfur, and easily oxidised sulfides. Samples were then dissolved by dropwise addition of a stoichiometric volume of 3 M HCl and 20% $SnCl_2$. The addition of stannous chloride was included to reduce any Fe^{3+} in the sample to prevent pyrite oxidation (Pruden and Bloomfield, 1968; Chanton and Martens, 1985). The insoluble fraction of the sediment was removed by vacuum filtration through a 0.22 µm polycarbonate filter.

The filtrate was then acidified by addition of 0.5 ml 6 M HCl to prevent the precipitation of tin oxides, followed by the addition of an excess of saturated $BaCl_2$ solution. The resulting $BaSO_4$ precipitate was removed by vacuum filtration. The dry solid was then cleaned as the pore fluid samples by addition of 2 ml 6 M HCl, followed by two rinses in 18.2 MΩ water, and analysed for sulfur isotopes (see Section 3.3 below). In order to remove any nitrate trapped within the barite lattice during barite precipitation (Bao, 2006), which may contaminate the $\delta^{18}O_{SO_4}$, the barite was dissolved and reprecipitated by addition of DTPA (Diethylenetriaminepentaacetic acid) and subsequent acidification. Samples were then cleaned as the pore fluid samples by addition of 2 ml 6 M HCl, followed by two rinses in 18.2 MΩ water. The $BaSO_4$ was then dried and prepared for analysis of $\delta^{18}O_{SO_4}$, and a second analysis of $\delta^{34}S_{SO_4}$. Sulfur isotopes were analysed a second time in order to check that the barite had been quantitatively reprecipitated, and sulfur (and therefore also oxygen) isotope fractionation had not occurred.

3.3. Sulfur isotope analyses

Barite samples of 390–460 µg were weighed with excess V_2O_5 in tin and then combusted in a Thermo HT1112 Elemental Analyzer, and introduced into a Delta V Plus gas source mass spectrometer as SO_2. Elemental Analyzer settings for the furnace and GC were 1030 °C, and 110 °C respectively, and carrier flow rates were 85 ml/min. Each run was preceded by two international standards (NBS-127, $\delta^{34}S = 20.3‰$ and IAEA-SO-6, $\delta^{34}S = -34.1‰$) and an internal barite standard (13‰). Samples were run in groups of 20 with 3 bracketing NBS-127, for which $\sigma < 0.3‰$. Results are reported in standard delta notation ($\delta^{34}S$) relative to Vienna Canyon Diabolo Troilite (VCDT).

3.4. Oxygen isotope analyses

Barite samples of 120–210 µg were added to silver capsules and baked at low temperature (40 °C) overnight to remove any adsorbed water. Samples were then pyrolized in a Temperature Conversion Elemental Analyzer and introduced into a Thermo Delta V Plus mass spectrometer as CO. Samples were run in duplicate or triplicate, and average and standard deviation of these replicate analyses are reported. Average 2σ was less than 0.4‰. Samples were run in groups of 20 with 3 bracketing NBS-127 ($\delta^{18}O_{SO_4} = 8.6‰$ – this value was determined in a multi-lab calibration and is reported in Brand et al., 2009) and a laboratory generated standard (EMB-$\delta^{18}O_{SO_4} = 15‰$). Results are reported in the standard delta notation ($\delta^{18}O$) relative to VSMOW (standard mean ocean water).

4. Results

Pore fluid $\delta^{18}O_{SO_4}$ and $\delta^{34}S_{SO_4}$ and the CAS $\delta^{18}O_{SO_4}$ and $\delta^{34}S_{SO_4}$ are shown in Table 1, and in Fig. 2, plotted with previously published ODP shipboard pore fluid sulfate concentrations (Shipboard Scientific Party, 1991a, 1991b, 1997). The $\delta^{34}S_{SO_4}$ of pore fluid sulfate increases at all sites as sulfate concentrations decrease (Fig. 2c). Sulfur isotopes in the pore fluid reach a maximum of 77‰ at 100 m in Site 821, 30‰ at 200 m in Site 807, and 51‰ at 100 m in Site 1003 (Fig. 2a). The $\delta^{18}O_{SO_4}$ in the pore fluid reaches 24‰ at all sites, initially coevolving with the pore fluid $\delta^{34}S_{SO_4}$ but ultimately reaching a constant isotopic value, as if reaching equilibrium with water (Fig. 2b – this behaviour of the oxygen isotopes in sulfate to reach an "apparent equilibrium" with water is a function of cell-internal sulfur cycling. The term "apparent equilibrium" comes from Wortmann et al., 2007). In all cores there is no correlation between the sulfur and oxygen isotope composition of CAS and the sulfur or oxygen isotopic composition of the pore fluid sulfate.

We compare our CAS $\delta^{18}O_{SO_4}$ and $\delta^{34}S_{SO_4}$ results to previously published $\delta^{18}O_{SO_4}$ and $\delta^{34}S_{SO_4}$ values from pelagic barite of the same age (Paytan et al., 2004; Turchyn and Schrag, 2006) by calculating ages of samples using the best available age models (usually shipboard biostratigraphic data – Fig. 3). We have recorrected the data from Turchyn and Schrag (2006) to the community-revised NBS 127 barite standard of 8.6‰ (Brand et al., 2009). Our data span the last 25 million years when there is little variability in the $\delta^{34}S_{SO_4}$ of marine barite, allowing us to explore positive and negative deviations of CAS $\delta^{34}S_{SO_4}$ from barite $\delta^{34}S_{SO_4}$. Over this timescale, the CAS $\delta^{34}S_{SO_4}$ is within ±2‰ of coeval barite at

Table 1
CAS.

Sample label	Sample type	Depth (mcd)	$\delta^{34}S$ (‰, VCDT)	$\delta^{18}O$ (‰ VSMOW)	Sample label	Sample type	Depth (mcd)	$\delta^{34}S$ (‰, VCDT)	$\delta^{18}O$ (‰ VSMOW)
807A_1H3_145-150	pore fluid sulfate	4.45	19.8	9.3	807A_1H3_145-150	CAS	4.45	20.9	10.5
807A_2H4_145-150	pore fluid sulfate	13.35	19.8	11.3	807A_2H4_145-150	CAS	13.35	21.0	10.6
807A_3H4_145-150	pore fluid sulfate	22.85	21.5	12.3	807A_3H4_145-150	CAS	22.85	20.5	11.0
807A_4H4_145-150	pore fluid sulfate	32.35	21.8	13.9	807A_4H4_145-150	CAS	32.35	20.7	11.1
807A_5H4_145-150	pore fluid sulfate	41.85	22.9	15.7	807A_5H4_145-150	CAS	41.85	21.1	10.3
807A_6H4_145-150	pore fluid sulfate	51.35	23.0	15.9	807A_6H4_145-150	CAS	51.35	21.1	11.7
807A_12H4_145-150	pore fluid sulfate	108.35	25.7	20.4	807A_9H4_145-150	CAS	79.85	21.3	11.6
807A_15H5_145-150	pore fluid sulfate	137.1	26.5	20.9	807A_12H4_145-150	CAS	108.35	21.3	11.9
807A_18H4_145-150	pore fluid sulfate	165.35	27.5	21.6	807A_15H5_145-150	CAS	137.1	20.5	12.9
807A_21H4_145-150	pore fluid sulfate	193.95	28.1	23.0	807A_18H4_145-150	CAS	165.35	21.7	12.6
807A_24H4_145-150	pore fluid sulfate	222.35	28.3	22.9	807A_21H4_145-150	CAS	193.85	21.5	12.2
807A_30X4_140-150	pore fluid sulfate	279.7	28.0	20.9	807A_24H4_145-150	CAS	222.35	21.7	14.2
807A_33X3_140-150	pore fluid sulfate	306.7	27.2	22.4	807A_27H4_145-150	CAS	250.85	22.4	12.3
807A_36X3_140-150	pore fluid sulfate	335.3	26.7	21.3	807A_30X4_140-150	CAS	279.7	20.5	12.7
807A_39X2_140-150	pore fluid sulfate	362.8	27.5	21.5	807A_33X3_140-150	CAS	306.7	20.4	12.9
807A_42X4_140-150	pore fluid sulfate	395.1	28.3	21.1	807A_36X3_140-150	CAS	335.3	23.2	15.8
807A_45X5_140-150	pore fluid sulfate	425.7	27.2	n.a.	807A_39X2_140-150	CAS	362.8	21.8	12.7
807A_48X3_140-150	pore fluid sulfate	451.5	27.5	n.a.	807A_42X4_140-150	CAS	395.1	22.1	11.2
807A_51X3_140-150	pore fluid sulfate	480.5	27.0	n.a.	807A_45X5_140-150	CAS	425.7	21.8	10.4
807A_54X4_0-10	pore fluid sulfate	509.6	32.9	n.a.	807A_48X3_140-150	CAS	451.5	21.6	9.9
807A_57X4_140-150	pore fluid sulfate	539.6	26.3	n.a.	807A_51X3_140-150	CAS	480.5	21.9	9.9
807A_60X4_140-150	pore fluid sulfate	568.5	25.3	n.a.	807A_54X4_0-10	CAS	509.6	21.8	10.3
821A_1H2_145-150	pore fluid sulfate	2.95	29.2	19.8	807A_57X4_140-150	CAS	539.6	21.7	11.7
821A_2H5_145-150	pore fluid sulfate	11.85	36.5	24.2	807A_60X4_140-150	CAS	568.5	21.2	10.4
821A_3H5_145-150	pore fluid sulfate	21.35	34.0	23.7	807A_63X4_0-10	CAS	596.1	20.8	9.2
821A_4H5_145-150	pore fluid sulfate	30.85	39.4	23.5	821A_1H2_145-150	CAS	2.95	21.3	11.1
821A_5H5_145-150	pore fluid sulfate	40.35	49.2	23.6	821A_2H5_145-150	CAS	11.85	20.7	11.0
821A_6H5_145-150	pore fluid sulfate	49.85	60.7	24.0	821A_3H5_145-150	CAS	21.35	21.7	11.0
821A_7H5_145-150	pore fluid sulfate	59.35	69.5	24.5	821A_4H5_145-150	CAS	30.85	21.9	11.5
821A_8H5_145-150	pore fluid sulfate	68.85	74.1	24.3	821A_5H5_145-150	CAS	40.35	23.6	12.1
821A_9H5_145-150	pore fluid sulfate	78.35	74.4	22.1	821A_6H5_145-150	CAS	49.85	22.7	11.2
821A_10H5_145-150	pore fluid sulfate	87.85	75.7	22.9	821A_7H5_145-150	CAS	59.35	25.5	12.2
821A_13H5_145-150	pore fluid sulfate	116.35	73.2	n.a.	821A_8H5_145-150	CAS	68.85	23.7	11.7
1003A_1H1_145-150	pore fluid sulfate	1.45	20.8	10.5	821A_9H5_145-150	CAS	78.35	24.8	11.6
1003A_3H5_145-150	pore fluid sulfate	23.95	20.7	11.2	821A_10H5_145-150	CAS	87.85	23.7	11.0
1003A_4H2_140-150	pore fluid sulfate	28.805	22.0	10.9	821A_13H5_145-150	CAS	116.35	24.8	12.8
1003A_5H5_140-150	pore fluid sulfate	42.88	20.9	11.2	821A_17X5_140-150	CAS	153.3	22.7	11.9
1003A_6H5_140-150	pore fluid sulfate	52.4	20.7	11.2	821A_20X5_140-150	CAS	182.3	22.8	11.6
1003A_7H5_140-150	pore fluid sulfate	61.49	21.1	12.9	821A_23X5_140-150	CAS	210.9	22.4	9.7
1003A_9H1_140-150	pore fluid sulfate	74.81	20.5	11.0	821A_26X5_140-150	CAS	239.6	21.4	10.2
1003A_12X2_140-150	pore fluid sulfate	94.785	22.2	11.2	821A_29X5_140-150	CAS	268.5	20.8	10.3
1003A_13X4_140-150	pore fluid sulfate	107.44	21.7	11.0	821A_33X5_140-150	CAS	306.95	22.4	10.8
1003A_17X4_125-150	pore fluid sulfate	145.35	21.5	11.9	821A_38X5_140-150	CAS	355.3	21.5	9.5
1003B_21X5_135-150	pore fluid sulfate	192.62	23.6	14.5	821A_38X5_140-150	CAS	355.3	21.0	9.6
					821A_41X4_140-150	CAS	382.7	20.0	10.0
					1003A_1H1_143-144.5	CAS	1.43	20.8	10.5
					1003A_3H5_143-145	CAS	23.93	20.7	11.2
					1003A_4H2_139-141	CAS	28.805	22.0	10.9
					1003A_5H5_138-141	CAS	42.88	20.9	11.2
					1003A_6H5_138-140	CAS	52.4	20.7	11.2
					1003A_7H5_139-140.5	CAS	61.49	21.1	12.9
					1003A_9H1_131-132.5	CAS	74.81	20.5	11.0
					1003A_12X2_138.5-140	CAS	94.785	22.2	11.2
					1003A_13X4_138-140	CAS	107.48	21.7	11.0
					1003A_17X4_133.5-135.5	CAS	145.735	21.5	11.9
					1003A_22H1_133.5-135	CAS	189.435	23.6	14.5

Sites 1003 and 807, except for one outlier at Site 1003 (Fig. 3a). At Site 821, however, the CAS $\delta^{34}S_{SO_4}$ is isotopically heavier by up to 4‰ in the first 120 m of the section.

The CAS $\delta^{18}O_{SO_4}$ records in all sites do not show similar trends to the barite $\delta^{18}O_{SO_4}$, record, and have values that are at times as much as 6‰ offset from the barite $\delta^{18}O_{SO_4}$ results. All three CAS records are in good agreement with each other for the first 0.5 Ma, where they are consistently 2.4‰ higher than modern seawater (seawater $\delta^{18}O_{SO_4}$ is 8.6 ± 0.4‰ (Brand et al., 2009) while CAS $\delta^{18}O_{SO_4}$ is 11 ± 0.4‰) and 3‰ higher than marine core top barite (Fig. 3b). There is one peak of similar magnitude and duration in Site 807 CAS $\delta^{18}O_{SO_4}$ and barite $\delta^{18}O_{SO_4}$, however these are 5 Ma offset from each other, and none of the published age models for Site 807 (Kroenke et al., 1991; Lyle et al., 1993; Schrag et al., 1995; Martin and Scher, 2004) change the record sufficiently to reconcile the two peaks.

5. Discussion

Our results show that CAS $\delta^{18}O_{SO_4}$ and $\delta^{34}S_{SO_4}$ are isotopically distinct from pore fluid sulfate – in other words the incorporation of porefluid sulfate during carbonate recrystallization has not been sufficient to render CAS $\delta^{18}O_{SO_4}$ and $\delta^{34}S_{SO_4}$ values that are isotopically deviated towards the pore fluid sulfate (Fig. 2). Moreover, there is good agreement between CAS $\delta^{34}S_{SO_4}$ and coeval barite $\delta^{34}S_{SO_4}$ in two core sites (807 and 1003), although CAS $\delta^{34}S_{SO_4}$ is elevated above barite $\delta^{34}S_{SO_4}$ in the first half of Site 821.

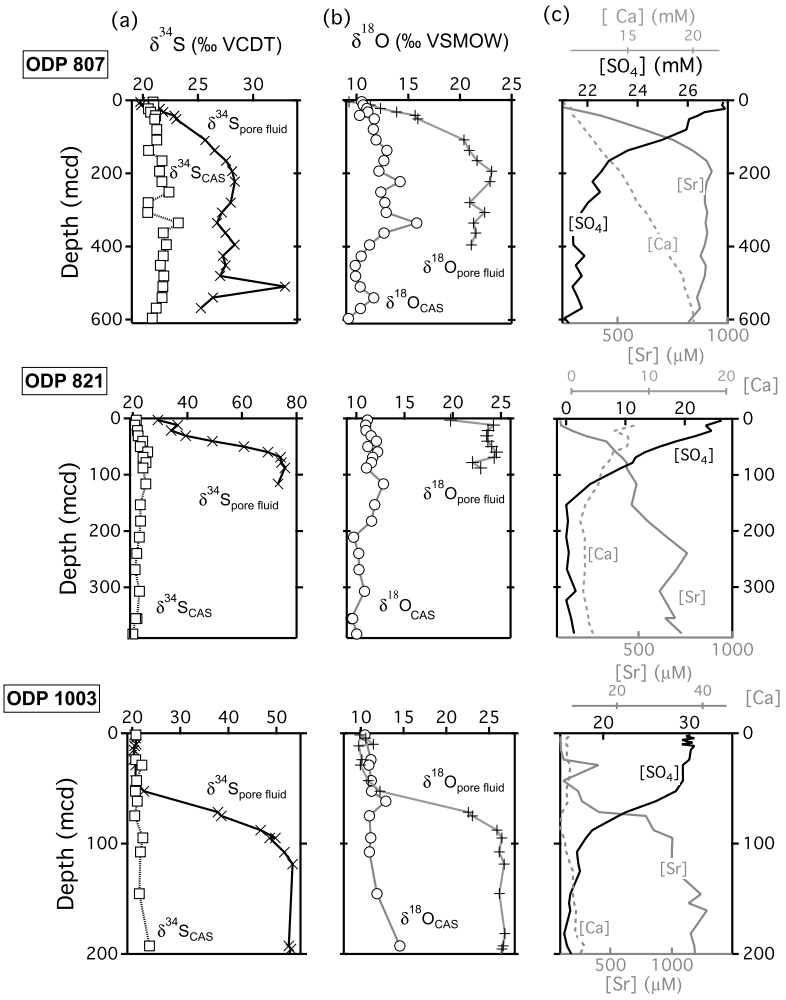

Fig. 2. The data for the three study sites. (a) Results of $\delta^{34}S_{SO_4}$ for pore fluid sulfate ((×) black line), and CAS ((□) grey line). (b) $\delta^{18}O_{SO_4}$ for pore fluid sulfate (+) and CAS $\delta^{18}O_{SO_4}$ (○) and (c) shipboard measurements of pore fluid sulfate concentrations (black line, top axis), calcium concentrations (dashed grey line, top axis) and strontium concentrations (grey line, bottom axis).

In contrast, CAS $\delta^{18}O_{SO_4}$ and barite $\delta^{18}O_{SO_4}$ do not have similar records for the whole of the studied interval.

5.1. Sulfur isotopes in carbonate associated sulfate

There are several factors that will determine whether marine diagenesis will impact the measured CAS $\delta^{34}S$. These include the amount of pore fluid sulfate that is incorporated into the reprecipitated carbonate (i.e. the partition coefficient of sulfate into recrystallizing carbonate – K_{SO_4}), the rate and extent of carbonate recrystallization, the original concentration of sulfate in the CAS, and the relative sulfur isotope difference between the original CAS $\delta^{34}S_{SO_4}$ and the $\delta^{34}S_{SO_4}$ of pore fluid sulfate. Additionally, although sulfate incorporation into biogenic carbonates has negligible sulfur isotope fractionation (Burdett et al., 1989), it is not known whether any sulfur isotope fractionation exists for sulfate incorporation into abiotic carbonate precipitated during marine diagenesis.

All three ODP sites studied have portions of their sediment columns where the carbonate sediments are in the presence of pore fluid that is isotopically distinct from the original carbonate, and from modern seawater. Site 821 is, however, the only site in which CAS $\delta^{34}S_{SO_4}$ significantly deviates from the 'predicted' sulfur isotope composition based on barite $\delta^{34}S_{SO_4}$. We hypothesize that this deviation may be due to pore fluid incorporation during marine diagenesis.

The rate of carbonate recrystallization and the partition coefficient of sulfate into carbonate are likely to have complementary effects on the potential alteration of CAS $\delta^{34}S_{SO_4}$ because the partition coefficient, K_{SO_4} should be dependent on calcite growth rate (Busenberg and Plummer, 1985). Higher rates of carbonate recrystallization incorporate more sulfate per unit of recrystallized carbonate, although it is unclear whether this relationship holds at the relatively slow rates experienced during early diagenesis in marine sediments. Values for K_{SO_4} in both primary and recrystallized carbonate, and their dependence on growth rate, are not well constrained. However, while the range of sulfate concentrations in biogenic carbonate can vary over several orders of magnitude (600–24 000 ppm – Staudt and Schoonen, 1995), the reported range of sulfate concentrations in diagenetic carbonate lies in a relatively narrow, and lower, range (200–600 ppm – Staudt and Schoonen, 1995).

The rate of carbonate recrystallization is arguably the dominant factor controlling pore fluid sulfate incorporation into carbonate, due to the likely dependence of K_{SO_4} on this rate. Numerous studies have calculated that mineral recrystallization rates decrease exponentially with increasing age (and, therefore, sediment depth – e.g. Richter and DePaolo, 1987). Broadly speaking, there exists an inverse relationship between reaction rate (R) and sediment age for both silicate and carbonate sediments and soils ($R = 0.1\ \mathrm{Age}^{-1}$ – Maher et al., 2004). This relationship extends

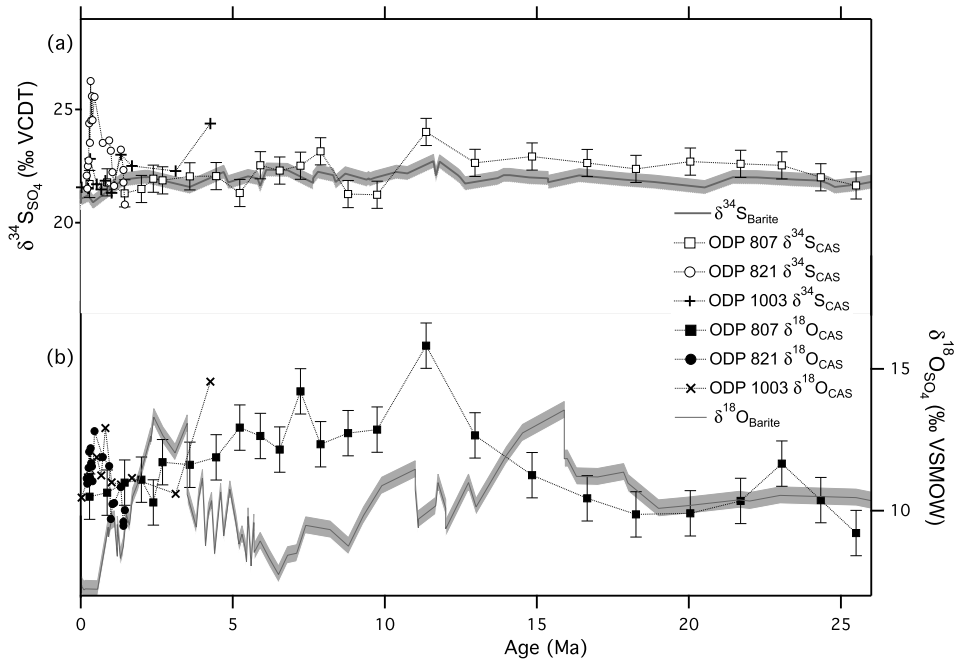

Fig. 3. (a) CAS $\delta^{34}S_{SO_4}$ results plotted against age for each site, using the best available age model ((□) ODP 807 – 0–14 Ma, Martin and Scher, 2004; 14–25 Ma, Schrag et al., 1995, (○) ODP 821 – Wei and Gartner, 1993, (+) ODP 1003 – Wright and Kroon, 2000). Barite $\delta^{34}S_{SO_4}$ for the same time interval (Paytan et al., 1998 – using an updated age model from Kurtz et al., 2003) is plotted at a grey line with a light grey bar showing the reported precision of ±0.2‰. (b) CAS $\delta^{18}O_{SO_4}$ results plotted against age for each site, using the best available age model ((■) ODP 807, (●) ODP 821, (×) ODP 1003). Barite $\delta^{18}O_{SO_4}$ for the same time interval (Turchyn and Schrag, 2006) is plotted at a grey line with a light grey bar showing the reported uncertainty of ±0.4‰. Error bars showing 2σ analytical uncertainty have been added to Site 807. Sites 1003 and 821 error bars have been omitted for visual clarity, however they are of the same order of magnitude.

over many orders of magnitude and types of environment, and has been shown to hold for young (<2 Ma) sedimentary carbonates (Fantle and DePaolo, 2007), although it breaks down on laboratory timescales (e.g. Burch et al., 1993) and in perturbed systems (e.g. Kirkwood and Nesbitt, 1991). For deep-sea sediments, like those we have studied, carbonate recrystallization rates can initially be very high in the uppermost sediments (~40% Myr^{-1} – Fantle and DePaolo, 2007), before dropping exponentially to ~2–3% in deeper sediments (Fantle and DePaolo, 2006, 2007). In such cases, if the partition coefficient of sulfate into carbonate does not vary significantly with depth, then it is the uppermost (i.e. youngest), most rapidly recrystallizing carbonate that will incorporate the most pore fluid sulfate. If this pore fluid sulfate is isotopically offset from seawater, then this has the potential to overprint the original CAS $\delta^{34}S_{SO_4}$.

The preservation of primary CAS $\delta^{34}S_{SO_4}$ is therefore more likely in sites with low sedimentation rates, such that the majority of carbonate recrystallization has occurred near the surface, above deeper horizons that may have isotopically altered pore fluid. Changes in the sulfur isotope composition of the pore fluid in older, deeper sediments are unlikely to have such a significant effect on CAS $\delta^{34}S_{SO_4}$ because in the deeper sediments the carbonate recrystallization rates are much lower. Our results reinforce this hypothesis, as any variability we observe in CAS $\delta^{34}S_{SO_4}$ is limited to the youngest sediments in the presence of evolved pore fluid and CAS $\delta^{34}S_{SO_4}$ is relatively unaffected by elevated $\delta^{34}S_{SO_4}$ in the pore fluid at deeper horizons (see below).

5.1.1. Carbonate recrystallization models

It is possible to apply a simple, time-intergrated mass balance model to an idealized sediment column to estimate the recrystallization rate and illustrate this conceptual idea of the importance of sedimentation rate on CAS $\delta^{34}S_{SO_4}$. This is overlays two separate processes within the sediment column, carbonate recrystallization rates, which we scale as a function of age (therefore depth – see below) versus sulfate reduction and pore fluid sulfur isotope evolution, which we prescribe and set fixed for an idealized sediment column. Assuming that there is no sulfur isotope fractionation upon the incorporation of sulfate into diagenetic calcite, that the rate of carbonate precipitation is equal to the rate of dissolution (e.g. Fantle and DePaolo, 2007), and that carbonate that is recrystallizing at every depth is the remaining primary carbonate (i.e. secondary calcite is not re-dissolved at greater depths – e.g. Delaney, 1989), the resultant CAS $\delta^{34}S_{SO_4}$ value for a given depth, j in the sediment, can be derived:

$$\delta^{34}S_{S_j} = \frac{\delta^{34}S_{S_0}C_{S_0}(1-\sum_{i=0}^{j} r_i) + \sum_{i=0}^{j}\delta^{34}S_{F_i}(C_{S_{F_i}}/C_{Ca_{F_i}})K_{SO_4}r_i}{C_{S_0}(1-\sum_{i=0}^{j} r_i) + \sum_{i=0}^{j}(C_{S_{F_i}}/C_{Ca_{F_i}})K_{SO_4}r_i} \quad (1)$$

In this equation, C_{S_0} is the concentration of sulfate in carbonate at the sediment-water interface – which is held constant, and K_{SO_4} is a function of the pore fluid sulfate/calcium ratio (e.g. Richer, 1996):

$$\left([SO_4^{2-}]/[Ca^{2+}]\right)_{calcite} = K_{SO_4}\left([SO_4^{2-}]/[Ca^{2+}]\right)_{pore\ fluid} \quad (2)$$

which is denoted at depth i as $C_{S_{F_i}}/C_{Ca_{F_i}}$. The $\delta^{34}S_{S_0}$ ($\delta^{34}S_{SO_4}$ in carbonate at the top of the sediment column) is that of modern seawater (21.1‰), r_i is the recrystallization rate (units $time^{-1}$) at depth i, which is related to age by sedimentation rate, and $\delta^{34}S_{F_i}$ is the isotopic composition of sulfate in the pore fluid at depth i.

This approach is similar to the "statement of diagenetic effect" from Fantle et al. (2010), Fantle (2010), with the exception that we assume that the sulfate concentrations between the solid and the fluid are not in equilibrium since they are driven by the 'external process' of sulfate reduction, and that there is no sulfur isotope fractionation upon sulfate incorporation into recrystallized carbonate (as with biogenic carbonate – Burdette et al., 1989). Moreover, because pore fluid sulfate concentrations are only negligibly by the addition of sulfate from dissolving carbonate, we set pore fluid sulfate concentrations and sulfur isotope compositions independently

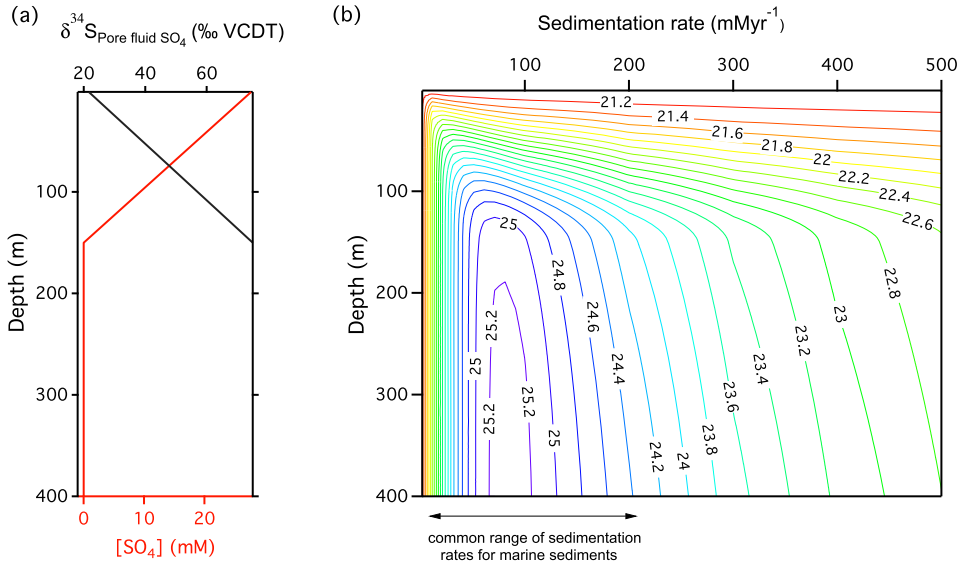

Fig. 4. (a) Modelled parameters used in the recrystallization model-pore fluid sulfate concentrations (red line, bottom axis) drop from seawater values to zero over the upper 150 m, while the sulfur isotopic composition of the sulfate ($\delta^{34}S_{SO_4}$, black line, top axis) evolves from seawater values to 75‰ over the same depth. (b) CAS $\delta^{34}S_{SO_4}$ results from the recrystallization model using a carbonate recrystallization rate $R = 0.4e^{-t/0.875}$. Results are shown as a contour plot where CAS $\delta^{34}S_{SO_4}$ values are plotted as lines of equal $\delta^{34}S_{SO_4}$, over the depth of the sediment and for a range of sedimentation rates (1–500 m Myr^{-1}). The maximum $\delta^{34}S_{SO_4}$ is 25.3‰ (4.2‰ elevated above seawater values) and occurs in sediments that have passed through the maximum pore fluid sulfur isotope composition at sedimentation rates from 50–150 m Myr^{-1}. These sedimentation rates are high enough that young, rapidly recrystallizing sediment is in contact with evolved pore fluid, but not so rapidly that they are recrystallized in contact with sulfate depleted pore fluid. (For interpretation of the references to colour in this figure legend, the reader is referred to the web version of this article.)

of the model. Finally, it is assumed that the pore fluid sulfate concentration and sulfur isotope profiles are in steady state and do not change over time. The latter assumption is potentially problematic, because the sulfate profile is controlled by microbial processes that may vary over time. However, this assumption is justified in the absence of further external constrains on the evolution of sulfate reduction rates in marine sediments over the most recent ~30 Ma.

We use our model with a hypothetical 400 m sediment column and an idealized pore fluid $\delta^{34}S_{SO_4}$ (Fig. 4) with sulfate concentrations decreasing from seawater concentrations to zero over the uppermost 150 m (Fig. 4a). We further assume that pore fluid calcium concentrations remain at seawater concentrations throughout the sediment column. This assumption is a simplification of the sedimentary system, because pore fluid calcium concentrations can both increase or decrease from seawater values (e.g. Sites 807 and 821 – see Fig. 2c). In our model, the partition coefficient is a function of the pore fluid sulfate/calcium ratio (Eq. (2)), and therefore this assumption will affect the amount of sulfate that is incorporated into the recrystallized calcite. However, this ratio (sulfate/calcium) is dominated in shallow marine sediments by sulfate concentrations decreasing by up to 30 mM, while the calcium concentrations typically (over this depth range) change by up to 5 mM. Therefore we take this simplification as acceptable for our purposes. In our hypothetical scenario, the exponential relationship between the recrystallization rate, R and depth is taken to be (from Fantle and DePaolo, 2007):

$$R(t) = 0.4e^{-t/0.865} \tag{3}$$

where t is the age of the sediment (time since deposition). We vary the sedimentation rate between a maximum of 500 and a minimum of 1 m Myr^{-1} and take the concentration of sulfate in the initial carbonate (Cs_i) at 1000 ppm (based on average foraminiferal concentrations from Staudt and Schoonen, 1995). We further assume an upper bound on the partition coefficient (K_{SO_4}) of 3.6×10^{-4}, such that the concentration of sulfate in the recrystallized calcite is equal to that of the original calcite at the top of the sediment column. Results of the model (Fig. 4b) are shown as a contour plot, with lines of equal CAS $\delta^{34}S_{SO_4}$ values over the depth of the sediment and for the range of modelled sedimentation rates. Our calculations suggest that CAS $\delta^{34}S_{SO_4}$ can be elevated above its initial $\delta^{34}S_{SO_4}$ by a maximum of about 4‰, and this only in sediments that have sedimentation rates from 50–150 m Myr^{-1}. This indicates that CAS $\delta^{34}S_{SO_4}$ will not deviate from primary seawater $\delta^{34}S_{SO_4}$ by more than a few permil over a large range of sedimentation rates, even with extreme pore fluid isotopic variance and high rates of carbonate recrystallization.

These results (Fig. 4b) suggest that, for a fixed depth distribution of carbonate recrystallization, and pore fluid sulfate evolution due to bacterial sulfate reduction, only sediments deposited at intermediate sedimentation rates are susceptible to diagenetic overprinting of CAS $\delta^{34}S_{SO_4}$. This is because the majority of carbonate recrystallization will occur in the youngest sediments. The relative position of the youngest sediment versus the zone of sulfate reduction (typically 50–150 mbsf) will determine whether diagenesis has a significant impact on the overall CAS $\delta^{34}S_{SO_4}$. When the $\delta^{34}S_{SO_4}$ of the pore fluid reaches its maximum values at the bottom of the zone of sulfate reduction, the pore fluid sulfate concentrations also reach their lowest concentrations, so very little of this highly evolved $\delta^{34}S_{SO_4}$ can be incorporated. Thus the critical region for CAS diagenesis is where there is relatively evolved sulfate $\delta^{34}S_{SO_4}$ in the presence of both high pore fluid sulfate concentrations, and high carbonate recrystallization rates. If sedimentation rates are low relative to the depth over which sulfate is depleted (~10 m Myr^{-1}), then young, highly reactive sediment will be in contact with isotopically unevolved pore fluid. At the other extreme, very rapid sedimentation rates (>300 m Myr^{-1}) will put reactive sediment below this critical region before sufficient recrystallization has occurred to overprint the original $\delta^{34}S_{SO_4}$. It is thus at sedimentation rates in the intermediate range (50–150 m) where carbonate recrystallization could impact the CAS $\delta^{34}S_{SO_4}$. The dependence of the diagenetic deviation of CAS $\delta^{34}S_{SO_4}$ on the sedimentation rate is particularly important in carbonates with low original sulfate concentrations, such as foraminiferal oozes or aragonitic sediments, which are not as buffered to the original $\delta^{34}S_{SO_4}$ of CAS, as are sediments with higher CAS concentrations (e.g. the Florida Keys, Lyons et al., 2004).

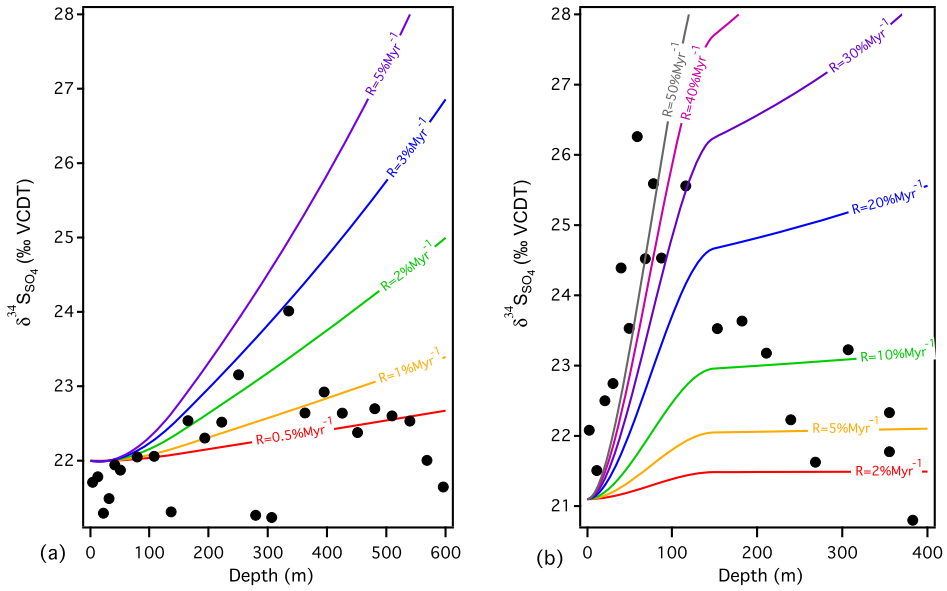

Fig. 5. Application of the recrystallization model applied to Site 807 (a) and 821 (b) using each site's known pore fluid conditions and primary CAS $\delta^{34}S_{SO_4}$ assumed from the marine barite curve (22‰ for 807 and 21.1‰ for 821). The projected CAS $\delta^{34}S_{SO_4}$ evolution with depth for different recrystallization rates are shown as different coloured lines, with black spheres to show the data. (For interpretation of the references to colour in this figure legend, the reader is referred to the web version of this article.)

For Site 807 and 821, we can use the known sedimentation rates and pore fluid $\delta^{34}S_{SO_4}$, sulfate and calcium concentrations, along with Eq. (1) to obtain a first order estimate of recrystallization rates. We do this by comparing the calculated CAS $\delta^{34}S_{SO_4}$ (as above) with measured CAS $\delta^{34}S_{SO_4}$ (Fig. 5), assuming sulfate concentrations of 1000 ppm, and a K_{SO_4} of 3.6×10^{-4}, as above. We chose to do these calculations for Sites 807 and 821 because Site 807 already has well characterized recrystallization rates (Fantle and DePaolo, 2006, 2007) and Site 821 is the site where we see isotopically distinct CAS, which could contain a diagenetic component. Site 1003 has complicated hydrology, which does not lend itself to this calculation. This calculation assumes that the modern pore fluid profiles measured at Sites 821 and 807 are at steady-state with respect to sulfate and calcium concentrations, and $\delta^{34}S_{SO_4}$. With regard to calcium concentrations, there is inherent uncertainty in the extent to which modern pore fluid profiles represents long-term pore fluid conditions. This is because the reactive length scale of calcium is much shorter than the sediment column in both sites (e.g. Fantle and DePaolo, 2007), such that pore fluid calcium concentrations are reset by reactions in the sediment, obscuring previous reactions or past advection. However, modern pore fluid concentrations represent our best hypothesis for pore fluid calcium concentrations over the past 0–30 Ma.

At Site 807 the best fit to our model suggests a carbonate recrystallization rate of 2–10% Myr^{-1} for the top 300 m of sediments (Fig. 5a), which is similar to the recrystallization rates in the upper most sediments calculated based on strontium concentrations and isotopes (2–3% Myr^{-1} – Fantle and DePaolo, 2006). In contrast, our model suggests Site 821 has carbonate recrystallization rates of 20–50% Myr^{-1} for the top 150 m. The estimate of recrystallization rates at Site 821 may be an overestimate, because we assume that only recrystallization occurs, when in fact this sediment is likely to also be experiencing net carbonate precipitation, as evidenced by a decrease in calcium concentrations over the uppermost 150 m at this Site. A similar time-dependent reactive transport model of strontium concentrations as was used in Site 807 (Fantle and DePaolo, 2006) could be applied to Site 821, however this is complicated by likely brine advection deeper in the sediment column, which may skew the lower strontium pore fluid profiles. If we look at the strontium pore fluid profiles from Sites 821 and 807, we see that both sites show similarly increasing strontium pore fluid concentrations with depth, although the sediments at Site 821 are much younger (2 Ma vs. 30 Ma) and contain less carbonate than at Site 807. This supports our previous calculation that recrystallization rates are much higher at Site 821 than Site 807, in order to produce such elevated pore fluid strontium concentrations in these younger sediments.

Our results suggest that the high uppermost carbonate recrystallization rates at Site 821 have a larger impact on CAS $\delta^{34}S_{SO_4}$ than the prolonged presence of elevated pore fluids $\delta^{34}S_{SO_4}$ at depth at Site 807. Finally, below 100 m the CAS $\delta^{34}S_{SO_4}$ at Site 821 return from values that are higher than coeval barite back to those we expect from primary calcite (Fig. 3a). This may be the result of variations in the pore fluid sulfate profile over time, for example if sulfate reduction rates were lower and the pore fluid less evolved 2 million years ago when the deeper sediments were at the top of the sediment column.

These results emphasize that a careful analysis of the depositional conditions is important in the selection of carbonate samples of CAS, to determine the potential influence of early marine diagenesis. Where possible, high density sampling of the same stratigraphic interval from more than one carbonate sequence will help to unpick possible diagenetic alteration from the global marine sulfate trends. Although our results are based on nanofossil oozes, which do not comprise the geological record before the Cretaceous, these results are broadly applicable in other micritic carbonate environments. This is because the relationship between sediment age and reaction rate (or recrystallization rate) is broadly similar across a variety of different mineral phases and diagenetic environments (Maher et al., 2004). Foraminiferal oozes do represent a "worst case scenario" for CAS preservation, however, because foraminiferal calcite has relatively low original sulfate concentrations (600–2000 ppm, Staudt and Schoonen, 1995), and so the original sulfate is less buffered to marine diagenesis. Other sediments which may be similarly problematic are aragonitic sediments which are recrystallizing to calcite, because it is thought that sulfate is more easily incorporated into calcite than aragonite (Kitano et al., 1975; Busenberg and Plummer, 1985). We also note that given the large range in marine sulfate concentrations over Earth history, it is likely that the effect of diagenetic overprinting on CAS $\delta^{34}S_{SO_4}$ may not be the same over time, as the concentra-

tion of sulfate in carbonate has likely also varied over time with sulfate concentrations.

5.1.2. Directly comparing CAS and barite $\delta^{34}S_{SO_4}$

Although our data suggest minimal diagenetic overprinting on CAS $\delta^{34}S_{SO_4}$, especially at Sites 1003 and 807, there is larger measured variability in the CAS $\delta^{34}S_{SO_4}$ compared to the barite $\delta^{34}S_{SO_4}$ (Fig. 3a). Even at low rates of recrystallization, it is possible that very small amount of pore fluid incorporation could increase the CAS $\delta^{34}S_{SO_4}$ above that expected from primary calcite alone. On the other hand, CAS $\delta^{34}S_{SO_4}$ that lies below the "expected values" is often attributed to contamination during extraction. For example, it has been shown that microcrystalline grains of pyrite will dissolve upon acid addition (Marenco et al., 2008); pyrite and other possible contaminants have a lower $\delta^{34}S_{SO_4}$ than the carbonate fraction. It is possible that, even with our care in extraction, contaminants have not been fully removed. Recently revised extraction techniques may be sufficient to remove the phases contributing to this variability (Wotte et al., 2012). However, organic sulfur compounds that are structurally bound within the carbonate lattice are unlikely to be removed by the extensive bleaching steps taken prior to carbonate dissolution. Our results support the idea that variations of <2‰ in CAS results should be treated with caution (this has been implied by other authors, e.g. Marenco et al., 2013).

5.2. Oxygen isotopes in carbonate associated sulfate

Previous work on CAS $\delta^{18}O_{SO_4}$ has shown that modern carbonate shells record a value that is consistent with seawater but with a variability of 2‰ or greater, which was ascribed to vital effects (Cortecci and Longinelli, 1971). Our results, however, show very little similarity to either modern seawater, or to the barite $\delta^{18}O_{SO_4}$ record over the past 25 Ma (Turchyn and Schrag, 2006). The core-top CAS $\delta^{18}O_{SO_4}$ measurements are 2.4‰ elevated above the accepted seawater $\delta^{18}O_{SO_4}$ value (8.6‰ – Brand et al., 2009). Core-top barite is isotopically offset from seawater by 1.4‰ (Turchyn and Schrag, 2004). Although an oxygen isotope fractionation between CAS $\delta^{18}O_{SO_4}$ and seawater sulfate may exist, this does not explain why there is no correlation between trends in the barite $\delta^{18}O_{SO_4}$ record and in that of the CAS $\delta^{18}O_{SO_4}$ record (Fig. 3b). The CAS $\delta^{18}O_{SO_4}$ results here show no relationship to the $\delta^{18}O_{SO_4}$ of the pore fluid in these sites (Figs. 2b, 3b). Additionally, if CAS $\delta^{18}O_{SO_4}$ has been overprinted by porefluid sulfate incorporation, then it would be expected that CAS $\delta^{34}S_{SO_4}$ would also show diagenetic overprinting, because both $\delta^{34}S_{SO_4}$ and $\delta^{18}O_{SO_4}$ become isotopically enriched at similar depths in the pore fluid.

The CAS $\delta^{18}O_{SO_4}$ and barite $\delta^{18}O_{SO_4}$ records are not easily reconciled by laboratory artefacts during CAS extraction, either by the liberation of non-CAS phases, or by sulfate–oxygen exchange. Non-CAS mineral phases are mostly in a reduced valence state (e.g. S^0, S^-, S^{2-}), and so will incorporate oxygen during oxidation, either from water from the laboratory (measured at −7‰) or dissolved molecular oxygen (~23‰). Our CAS $\delta^{18}O_{SO_4}$ is largely isotopically heavier than the coeval barite $\delta^{18}O_{SO_4}$, which would require that our measured signal contained significant (~40%) reduced sulfur phases that were oxidised using dissolved molecular oxygen (Fig. 6). This requires that ~40% of the CAS $\delta^{34}S_{SO_4}$ is also sourced from sulfur that is oxidised during extraction. Reduced sedimentary sulfur phases commonly have a lower sulfur isotope composition than marine sulfate. However, for the samples where CAS $\delta^{18}O_{SO_4}$ does not agree with barite $\delta^{18}O_{SO_4}$, there is good agreement between the sulfur isotope composition of CAS and barite, either suggesting minimal contribution from reduced sulfur phases, or that reduced sulfur phases in these different cores all had $\delta^{34}S$ values that were similar to marine sulfate. The latter

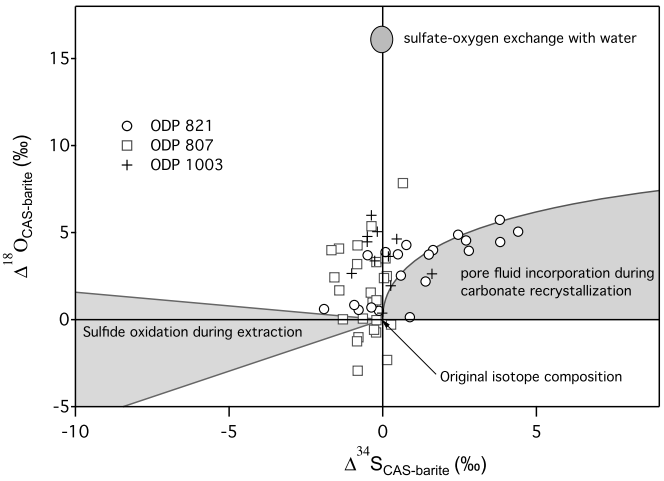

Fig. 6. Summary of all the bulk CAS data, plotted as the difference between each CAS $\delta^{34}S_{SO_4}$ and $\delta^{18}O_{SO_4}$ result, and coeval barite $\delta^{34}S_{SO_4}$ and $\delta^{18}O_{SO_4}$. Shown in grey in the upper right-hand quadrant, is the region of values expected during carbonate recrystallization in contact with isotopically evolved pore fluid (modelled from the idealized pore fluid profile in Fig. 4(a)), using a maximum sedimentation rate of 200 m Myr^{-1}, and a maximum recrystallization rate of 80% Myr^{-1}. The grey region on the left-hand side is that expected from sulfide oxidation, assuming a $\delta^{34}S$ of −20‰ and a water $\delta^{18}O_{H_2O}$ of −7‰, a $\delta^{18}O_{O_2}$ for atmospheric oxygen of 23‰ (upper grey line). The CAS $\delta^{34}S_{SO_4}$ results plot near the origin (no difference from coeval barite $\delta^{34}S_{SO_4}$) except for some samples for Site 821, which are in the "pore fluid recrystallization" field. The CAS $\delta^{18}O_{SO_4}$ do not plot closely to the origin, highlighting that bulk CAS $\delta^{18}O_{SO_4}$ and barite $\delta^{18}O_{SO_4}$ results do not match well for any of the record. The expected value for the oxygen isotope exchange of sulfate with water is also shown, assuming a 23‰ isotope fractionation factor as calculated by Zeebe, 2010.

scenario would be unusual, and we therefore argue that extraction artefacts are unlikely to be the explanation for discrepancies between CAS $\delta^{18}O_{SO_4}$ and barite $\delta^{18}O_{SO_4}$.

We also consider it unlikely that sulfate oxygen isotopes have exchanged with water or other oxygen-bearing phases during precipitation, burial or extraction. Previous laboratory experiments (Hoering and Kennedy, 1957; Chiba and Sakai, 1985) indicate that exchange is unlikely to occur in the pH and temperature ranges at which the carbonate existed, or was subsequently analysed. Moreover, if sulfate–oxygen exchange with water is responsible for deviations in the CAS $\delta^{18}O_{SO_4}$, then all the CAS $\delta^{18}O_{SO_4}$ results should be higher than the original barite $\delta^{18}O_{SO_4}$, as sulfate–oxygen isotope exchange with water has a calculated and measured fractionation of +23 to +38‰ (Mizutani and Rafter, 1969; Lloyd, 1968; Zeebe, 2010).

It is, however, possible that sulfate incorporation into carbonate needs to be understood differently for sulfur versus oxygen isotopes. The role of biology in the incorporation of sulfate into biogenic carbonates, for example, remains enigmatic. It is likely that the oxygen atoms in a sulfate molecule are impacted more than the central sulfur atom when sulfate is incorporated into carbonate, because of their proximity to the calcium ion at the site of structural substitution. This has the potential to result in the isotope fractionation of sulfate–oxygen associated with this ionic interaction, without resulting in a sulfur isotope fractionation. Secondly, it is possible that microenvironments undergoing biogenic calcification could have $\delta^{18}O_{SO_4}$ values that are modified from seawater due to microbial processes locally that facilitate oxygen isotope exchange between sulfate and water.

To date, oxygen isotope fractionation during sulfate incorporation into carbonate, and the specifics of any vital effects, remain unconstrained. In bulk carbonate samples such as those presented here it is not possible to address these questions further. Variations in CAS $\delta^{18}O_{SO_4}$ do show interesting trends at significant time intervals, which are larger than the variability we see over the last

25 million years and may be representative of global variations in the sulfur cycle (Newton et al., 2004). Even if it is the case that $\delta^{18}O_{SO_4}$ is not always representative of a global environment, variations in $\delta^{18}O_{SO_4}$ are still illuminating aspects of the dynamics of an interesting and important microenvironment, which merits closer attention.

6. Conclusions

Carbonate-associated sulfate results record similar sulfur isotope values to marine barite, but with more variability, resulting in an uncertainty that is much greater than the analytical uncertainty. Carbonate-associated sulfate is also prone to overprinting by carbonate recrystallization when sedimentation rates and bacterial sulfate reduction rates are elevated sufficiently to introduce rapidly recrystallizing carbonate (<2 Ma) into highly evolved pore fluid. We used a model to show, however, that the deviation of the sulfur isotope composition of CAS will not differ from seawater by more than 4‰ over a range of sedimentation and carbonate recrystallization rates.

Oxygen isotopes of carbonate-associate sulfate are more complex than sulfur isotopes and do not appear to record the same signal as marine barite $\delta^{18}O_{SO_4}$. Despite these uncertainties, CAS $\delta^{18}O_{SO_4}$, is still a powerful tool, at the least to assess the likelihood of sulfide oxidation during CAS extraction. In the cases where CAS $\delta^{18}O_{SO_4}$ and $\delta^{34}S_{SO_4}$ are not representative of the global ocean, they still have potential to yield interesting information on sedimentary processes or specific microenvironments. Careful sedimentary characterization and high density sampling at multiple sites is vital to distinguish between CAS results showing local diagenetic trends and those that are basin-wide or global.

Acknowledgements

We would like to thank Rob Newton, Pedro Marenco and Matt Fantle for their reviews, which have greatly improved the manuscript, and Ben Brunner and Tim Lyons for their advice and invaluable insight. We are also indebted to James Rolfe, Jenny Roberts, Gilad Antler, Claire Hedgecott and Tim Craig for technical assistance. This work was supported by a NERC Studentship (award code NE/H52449X/1).

References

Baker, P.A., Gieskes, J.M., Elderfield, H., 1982. Diagenesis of carbonates in deep-sea sediments – evidence from Sr/Ca ratios and interstitial dissolved Sr^{2+} data. J. Sediment. Petrol. 52, 71–82.

Bao, H.M., 2006. Purifying barite for oxygen isotope measurement by dissolution and reprecipitation in a chelating solution. Anal. Chem. 78, 304–309.

Berner, R.A., 1987. Models for carbon and sulfur cycles and atmospheric oxygen – application to paleozoic geologic history. Am. J. Sci. 287, 177–196.

Berner, R.A., Canfield, D.E., 1989. A new model for atmospheric oxygen over Phanerozic time. Am. J. Sci. 189, 333–361.

Brand, W.A., Coplen, T.B., Aerts-Bijma, A.T., Böhlke, J.K., Gehre, M., Geilmann, H., Gröning, M., Jansen, H.G., Meijer, H.A.J., Mroczkowski, S.J., Qi, H., Soergel, K., Stuart-Williams, H., Weise, S.M., Werner, R.A., 2009. Comprehensive inter-laboratory calibration of reference materials for $\delta^{18}O$ versus VSMOW using various on-line high-temperature conversion techniques. Rapid Commun. Mass Spectrom. 23, 999–1019.

Brunner, B., Bernasconi, S.M., Kleikemper, J., Schroth, M.H., 2005. A model for oxygen and sulfur isotope fractionation in sulfate during bacterial sulfate reduction processes. Geochim. Cosmochim. Acta 69, 4773–4785.

Burch, T.E., Nagy, K.L., Lasaga, A.C., 1993. Free-energy dependence of albite dissolution kinetics at 80 °C and pH 8.8. Chem. Geol. 105, 137–162.

Burdett, J.W., Arthur, M.A., Richardson, M., 1989. A Neogene seawater sulfur isotope age curve from calcareous Pelagic microfossils. Earth Planet. Sci. Lett. 94, 189–198.

Busenberg, E., Plummer, L.N., 1985. Kinetic and thermodynamic factors controlling the distribution of SO_4^{2-} and Na^+ in calcites and selected aragonites. Geochim. Cosmochim. Acta 49, 713–725.

Canfield, D.E., 1998. A new model for Proterozoic ocean chemistry. Nature 396, 450–453.

Canfield, D.E., 2005. The early history of atmospheric oxygen: homage to Robert M. Garrels. Annu. Rev. Earth Planet. Sci. 33, 1–36.

Chanton, J.P., Martens, C.S., 1985. The effects of heat and stannous chloride addition on the active distillation of acid volatile sulfide from pyrite-rich marine sediment samples. Biogeochemistry 1, 375–383.

Chiba, H., Sakai, H., 1985. Oxygen isotope exchange-rate between dissolved sulfate and water at hydrothermal temperatures. Geochim. Cosmochim. Acta 49, 993–1000.

Claypool, G.E., Holser, W.T., Kaplan, I.R., Sakai, H., Zak, I., 1980. The age curves of sulfur and oxygen isotopes in marine sulfate and their mutual interpretation. Chem. Geol. 28, 199–260.

Cortecci, G., Longinelli, A., 1971. O-18/O-16 ratios in sulfate from living marine organisms. Earth Planet. Sci. Lett. 11, 273.

Delaney, M.L., 1989. Temporal changes in interstitial water chemistry and calcite recrystallization in Marine-Sediments. Earth Planet. Sci. Lett. 95, 23–37.

Fantle, M.S., DePaolo, D.J., 2006. Sr isotopes and pore fluid chemistry in carbonate sediment of the Ontong Java Plateau: calcite recrystallization rates and evidence for a rapid rise in seawater Mg over the last 10 million years. Geochim. Cosmochim. Acta 70, 3883–3904.

Fantle, M.S., DePaolo, D.J., 2007. Ca isotopes in carbonate sediment and pore fluid from ODP Site 807A: the Ca^{2+}_{aq}-calcite equilibrium fractionation factor and calcite recrystallization rates in Pleistocene sediments. Geochim. Cosmochim. Acta 71, 2524–2546.

Fantle, M.S., Maher, K.M., DePaolo, D.J., 2010. Isotopic approaches for quantifying the rates of marine burial diagenesis. Rev. Geophys. 48, RG3002.

Fantle, M.S., 2010. Evaluating the Ca isotope proxy. Am. J. Sci. 310, 194–230.

Fike, D.A., Grotzinger, J.P., 2008. A paired sulfate-pyrite delta S-34 approach to understanding the evolution of the Ediacaran–Cambrian sulfur cycle. Geochim. Cosmochim. Acta 72, 2636–2648.

Fritz, P., Basharmal, G.M., Drimmie, R.J., Ibsen, J., Qureshi, R.M., 1989. Oxygen isotope exchange between sulfate and water during bacterial reduction of sulfate. Chem. Geol. 79, 99–105.

Gellatly, A.M., Lyons, T.W., 2005. Trace sulfate in mid-Proterozoic carbonates and the sulfur isotope record of biospheric evolution. Geochim. Cosmochim. Acta 69, 3813–3829.

Gill, B.C., Lyons, T.W., Frank, T.D., 2008. Behavior of carbonate-associated sulfate during meteoric diagenesis and implications for the sulfur isotope paleoproxy. Geochim. Cosmochim. Acta 72, 4699–4711.

Gill, B.C., Lyons, T.W., Saltzman, M.R., 2007. Parallel, high-resolution carbon and sulfur isotope records of the evolving Paleozoic marine sulfur reservoir. Palaeogeogr. Palaeoclimatol. Palaeoecol. 256, 156–173.

Gill, B.C., Lyons, T.W., Shim, M., Hurtgen, M., Kah, L., Frank, T.D., 2005. Carbonate-associated sulfate as a tracer of ancient seawater chemistry. Abstr. Pap. – Am. Chem. Soc. 229, U890.

Higgins, J.A., Schrag, D.P., 2012. Records of Neogene seawater chemistry and diagenesis in deep-sea carbonate sediments and pore fluids. Earth Planet. Sci. Lett. 357, 386–396.

Hoering, T.C., Kennedy, J.W., 1957. The exchange of oxygen between sulfuric acid and water. J. Am. Chem. Soc. 79, 56–60.

Holland, H.D., 1984. The Chemical Evolution of the Atmosphere and the Oceans. Princeton University Press.

Holser, W.T., Schidlowski, M., Mackenzie, F.T., Maynard, J.B., 1988. Geochemical cycles of carbon and sulfur. In: Gregor, C.B., Garrels, R.M., Mackenzie, F.T., Maynard, J.B. (Eds.), Chemical Cycles in the Evolution of the Earth. John Wiley, pp. 105–173.

Hurtgen, M.T., Arthur, M.A., Suits, N.S., Kaufman, A.J., 2002. The sulfur isotopic composition of Neoproterozoic seawater sulfate: implications for a snowball Earth?. Earth Planet. Sci. Lett. 203, 413–429.

Kah, L.C., Lyons, T.W., Frank, T.D., 2004. Low marine sulphate and protracted oxygenation of the proterozoic biosphere. Nature 431, 834–838.

Kampschulte, A., Bruckschen, P., Strauss, H., 2001. The sulphur isotopic composition of trace sulphates in Carboniferous brachiopods: implications for coeval seawater, correlation with other geochemical cycles and isotope stratigraphy. Chem. Geol. 175, 149–173.

Kampschulte, A., Strauss, H., 2004. The sulfur isotopic evolution of Phanerozoic seawater based on the analysis of structurally substituted sulfate in carbonates. Chem. Geol. 204, 255–286.

Kasten, S., Jorgensen, B.B., 2000. Sulfate reduction in marine sediments. In: Schulz, H.D., Zabel, M. (Eds.), Marine Geochemistry, pp. 263–275.

Kirkwood, D.H., Nesbitt, H.W., 1991. Formation and evolution of soils from an acidified watershed: Plastic Lake, Ontario, Canada. Geochim. Cosmochim. Acta 55, 1295–1308.

Kitano, Y., Okumura, M., Idogaki, M., 1975. Incorporation of sodium, chloride and sulfate with calcium carbonate. Geochem. J. 84, 75–84.

Kroenke, L.W., Berger, W.H., Janecek, T.R., et al., 1991. Site 807. In: Kroenke, L.W., Berger, W.H., Janecek, T.R., et al. (Eds.), Proc. ODP. Initial Reports. In: Ocean Drilling Program, vol. 130, pp. 369–493.

Kurtz, A.C., Kump, L.R., Arthur, M.A., Zachos, J.C., Paytan, A., 2003. Early Cenozoic decoupling of the global carbon and sulfur cycles. Paleoceanography 18, 1090. http://dx.doi.org/10.1029/2003PA000908.

Lloyd, R.M., 1968. Oxygen isotope behavior in the sulfate-water system. J. Geophys. Res. 73, 6099–6110.

Lyle, M.W., Mayer, R.H., Larry, A., 1993. Detailed stratigraphic correlation of the Neogene sedimentary sequences on the Ontong Java Plateau by well logging: ODP Sites 803, 806, 807 and DSDP Site 586. In: Berger, W.H., Kroenke, L.W., Mayer, L.A., et al. (Eds.), Proc. ODP, Sci. Res., College Station TX 130, pp. 587–606.

Lyons, T.W., Walter, L.M., Gellatly, A.M., Martini, A.M., Blake, R.E., 2004. Sites of anomalous organic remineralization in the carbonate sediments of South Florida, USA: the sulfur cycle and carbonate-associated sulfate. In: Amend, J.P., Edwards, K.E., Lyons, T.W. (Eds.), Sulfur Biogeochemistry – Past and Present, pp. 161–176.

Maher, K., DePaolo, D.J., Lin, J.C.F., 2004. Rates of silicate dissolution in deep-sea sediment: in situ measurement using U-234/U-238 of pore fluids. Geochim. Cosmochim. Acta 68, 4629–4648.

Maher, K., Steefel, C.I., DePaolo, D.J., Viani, B.E., 2006. The mineral dissolution rate conundrum: insights from reactive transport modeling of U isotopes and pore fluid chemistry in marine sediments. Geochim. Cosmochim. Acta 70, 337–363.

Marenco, P.J., Corsetti, F.A., Hammond, D.E., Kaufman, A.J., Bottjer, D.J., 2008. Oxidation of pyrite during extraction of carbonate associated sulfate. Chem. Geol. 247, 124–132.

Marenco, P.J., Marenco, K.N., Lubitz, R.L., Niu, D., 2013. Contrasting long-term global and short-term local redox proxies during the Great Ordovician Biodiversification Event: a case study from Fossil Mountain, Utah, USA. Palaeogeogr. Palaeoclim. Palaeoecol. 377, 45–51.

Martin, E.E., Scher, H.D., 2004. Preservation of seawater Sr and Nd isotopes in fossil fish teeth: bad news and good news. Earth Planet. Sci. Lett. 220, 25–39.

Mizutani, Y., Rafter, T.A., 1969. Oxygen isotopic composition of sulphates. 3. Oxygen isotopic fractionation in bisulphate ion–water system. New Zeal. J. Sci. 12, 54–59.

Mizutani, Y., Rafter, T.A., 1973. Isotopic behaviour of sulphate oxygen in the bacterial reduction of sulphate. Geochem. J. 6, 183–191.

Newton, R.J., Pevitt, E.L., Wignall, P.B., Bottrell, S.H., 2004. Large shifts in the isotopic composition of seawater sulphate across the Permo-Triassic boundary in northern Italy. Earth Planet. Sci. Lett. 218, 331–345.

Paytan, A., Kastner, M., Campbell, D., Thiemens, M.H., 1998. Sulfur isotopic composition of Cenozoic seawater sulfate. Science 282, 1459–1462.

Paytan, A., Kastner, M., Campbell, D., Thiemens, M.H., 2004. Seawater sulfur isotope fluctuations in the cretaceous. Science 304, 1663–1665.

Pingitore, N.E., Meitzner, G., Love, K.M., 1995. Identification of sulfate in natural carbonates by X-ray-absorption spectroscopy. Geochim. Cosmochim. Acta 59, 2477–2483.

Pruden, G., Bloomfie, C., 1968. Determination of Iron(2) sulphide in soil in presence of Iron(3) oxide. Analyst 93, 532–534.

Richter, F.M., 1996. Models for the coupled Sr-sulfate budget in deep-sea carbonates. Earth Planet. Sci. Lett. 141, 199–211.

Richter, F.M., DePaolo, D.J., 1987. Numerical-models for diagenesis and the Neogene Sr isotopic evolution of seawater from Dsdp Site 590b. Earth Planet. Sci. Lett. 83, 27–38.

Schrag, D.P., DePaolo, D., Richter, F.M., 1995. Age and oxygen isotope data for bulk carbonate from ODP Site 130–807. Geochim. Cosmochim. Acta 59, 2265–2287.

Shipboard Scientific Party, 1991a. Site 807. In: Kroenke, L.W., Berger, W.H., Janecek, T.R. (Eds.), Proc. ODP, Init. Repts. Ocean Drilling Program, College Station, TX, pp. 369–493.

Shipboard Scientific Party, 1991b. Site 821. In: Davies, P.J., Mckenzie, J.A., Palmer-Julson, A. (Eds.), Proc. ODP, Init. Repts. Ocean Drilling Program, College Station, TX, pp. 569–614.

Shipboard Scientific Party, 1997. Site 1003. In: Eberli, G.P., Swart, P.K., Malone, M.J. (Eds.), Proc. Odp. Init. Repts. Ocean Drillin Program, College Station, TX, pp. 71–151.

Staudt, W.J., Schoonen, M.A.A., 1995. Sulfate incorporation into sedimentary carbonates. ACS Symp. Ser. 612, 332–345.

Symonds, P.A., Davies, P.J., Parisi, A., 1983. Structure and stratigraphy of the central Great Barrier Reef. BMR J. Aust. Geol. Geophys. 8, 277–291.

Takano, B., 1985. Geochemical implications of sulfate in sedimentary carbonates. Chem. Geol. 49, 393–403.

Turchyn, A.V., Schrag, D.P., 2004. Oxygen isotope constraints on the sulfur cycle over the past 10 million years. Science 303, 2004–2007.

Turchyn, A.V., Schrag, D.P., 2006. Cenozoic evolution of the sulfur cycle: insight from oxygen isotopes in marine sulfate. Earth Planet. Sci. Lett. 241, 763–779.

Wei, W., Gartner, S., 1993. Neogene calcerous nannofossil datums of ODP Site 133–821. In: Mckenzie, J.A., Davies, P.J., Palmer-Julson, A. (Eds.), Proc. ODP, Sci. Results. Ocean Drilling Program, College Station, TX, pp. 19–37.

Wortmann, U.G., Chernyavsky, B., Bernasconi, S.M., Brunner, B., Bottcher, M.E., Swart, P.K., 2007. Oxygen isotope biogeochemistry of pore water sulfate in the deep biosphere: dominance of isotope exchange reactions with ambient water during microbial sulfate reduction (ODP Site 1130). Geochim. Cosmochim. Acta 71, 4221–4232.

Wotte, T., Shields-Zhou, G.A., Strauss, H., 2012. Carbonate-associated sulfate: experimental comparisons of common extraction methods and recommendations toward a standard analytical protocol. Chem. Geol. 326, 132–144.

Wright, J.D., Kroon, D., 2000. Planktonic foraminiferal biostratigraphy of Leg 166. In: Eberli, G.P., Swart, P.K., Malone, M.J. (Eds.), Proc. ODP. Sci. Results. Ocean Drilling Program, College Station, TX.

Zeebe, R.E., 2010. A new value for the stable oxygen isotope fractionation between dissolved sulfate ion and water. Geochim. Cosmochim. Acta 74, 818–828.